Research Square

Preprints are preliminary reports that have not undergone peer review.
They should not be considered conclusive, used to inform clinical practice,
or referenced by the media as validated information.

Comprehensive methylome-wide association study with methylation-based WGCNA profiling and functional enrichment analyses in drug-induced liver injury

Romina Lorena de los Santos-Fernández
Servicio de Aparato Digestivo y Farmacología clínica, Instituto de Investigación Biomédica de Málaga-IBIMA Plataforma BIONAND, Hospital Universitario Virgen de la Victoria, Universidad de Málaga

Guillermo Paz-López
Bioinformatics Platform, Biomedical Research Institute of Malaga and Platform in Nanomedicine – IBIMA-BIONAND

Hao Niu
Servicio de Aparato Digestivo y Farmacología clínica, Instituto de Investigación Biomédica de Málaga-IBIMA Plataforma BIONAND, Hospital Universitario Virgen de la Victoria, Universidad de Málaga

Ismael Álvarez-Álvarez
Servicio de Aparato Digestivo y Farmacología clínica, Instituto de Investigación Biomédica de Málaga-IBIMA Plataforma BIONAND, Hospital Universitario Virgen de la Victoria, Universidad de Málaga

Irene Díaz-Alberola
Servicio de Aparato Digestivo y Farmacología clínica, Instituto de Investigación Biomédica de Málaga-IBIMA Plataforma BIONAND, Hospital Universitario Virgen de la Victoria, Universidad de Málaga

Judith Sanabria-Cabrera
Servicio de Aparato Digestivo y Farmacología clínica, Instituto de Investigación Biomédica de Málaga-IBIMA Plataforma BIONAND, Hospital Universitario Virgen de la Victoria, Universidad de Málaga

Marina Villanueva-Paz
Servicio de Aparato Digestivo y Farmacología clínica, Instituto de Investigación Biomédica de Málaga-IBIMA Plataforma BIONAND, Hospital Universitario Virgen de la Victoria, Universidad de Málaga

Andrés González-González
Bioinformatics Platform, Biomedical Research Institute of Malaga and Platform in Nanomedicine – IBIMA-BIONAND

Camilla Stephens
Servicio de Aparato Digestivo y Farmacología clínica, Instituto de Investigación Biomédica de Málaga-IBIMA Plataforma BIONAND, Hospital Universitario Virgen de la Victoria, Universidad de Málaga

M Isabel Lucena
lucena@uma.es

Servicio de Aparato Digestivo y Farmacología clínica, Instituto de Investigación Biomédica de Málaga-IBIMA Plataforma BIONAND, Hospital Universitario Virgen de la Victoria, Universidad de Málaga

Inmaculada Medina-Cáliz
Servicio de Aparato Digestivo y Farmacología clínica, Instituto de Investigación Biomédica de Málaga-IBIMA Plataforma BIONAND, Hospital Universitario Virgen de la Victoria, Universidad de Málaga

Raúl J Andrade
Servicio de Aparato Digestivo y Farmacología clínica, Instituto de Investigación Biomédica de Málaga-IBIMA Plataforma BIONAND, Hospital Universitario Virgen de la Victoria, Universidad de Málaga

---

Research Article

Keywords: Liver injury, metabolic dysfunction associated steatotic liver disease (MASLD), epigenetics, DNA methylation, pharmacogenomics

Posted Date: June 11th, 2026

DOI: https://doi.org/10.21203/rs.3.rs-9038512/v1

License: This work is licensed under a Creative Commons Attribution 4.0 International License. Read Full License

Additional Declarations: No competing interests reported.

Abstract

Background

Idiosyncratic drug-induced liver injury (DILI) is a rare, unpredictable and host-specific immune-mediated adverse reaction to drugs, herbal and dietary supplements. DILI is a complex disease whose presentation is influenced by multiple host and environmental factors. The latter modulate gene expression through epigenetic regulatory mechanisms, such as DNA methylation. This methylome-wide association study aims to characterise DILI differential methylation profile and to determine the disease mechanisms affected by DNA methylation dysregulation.

Methods

Whole blood DNA samples from 32 DILI patients and 33 healthy controls included in the Spanish DILI Registry were analysed using the Infinium MethylationEPIC 850k BeadChip microarray to screen differentially methylated CpG positions. After methylation data quality control, differentially methylated CpG sites or positions (DMPs) and regions (DMRs) analyses were conducted. Additionally, a DNA methylation-based weighted gene correlation network analysis (WGCNA) was performed with CpG sites nearby the gene transcription start site (TSS) to characterise clusters of functionally related genes based on their DNA methylation profiles. Functional and tissue enrichment analyses were performed to identify the processes and the target tissues affected by differential methylation in DILI.

Results

Global hypomethylation was observed in DILI. Hypomethylated DMR1 in *ENSG00000298543* was the most significant (HMFDR = 3.43×10^{-5}). *ENSG00000298543* encodes a long non-coding RNA antisense to CD58 and IGSF3, indicating DMR1 potential role in enhancing the immune response. Two gene modules with significant differential methylation were identified. ME1 was the most significant and the main methylation pattern in DILI (FDR = 1.29×10^{-10}). Meanwhile, ME0 (FDR = 7.13×10^{-5}) was a male-specific DILI module. Hypermethylated *MIR342* in ME1 suggested possible shared mechanisms with metabolic dysfunction-associated steatotic liver disease (MASLD). Functional enrichment analyses have shown the relevance of the sensory receptor signalling pathways and the immune response activation.

Conclusions

Altered DNA methylation was observed across samples, indicating genomic instability as a disease determinant in DILI. Additionally, DNA methylation profiling near the TSS region revealed DNA methylation participation in the regulation of the sensory signalling pathways and in the immune system overactivation, and evidenced the interaction between DNA methylation and non-coding RNAs. Moreover, this study demonstrated possible shared epigenetic features with other liver diseases, such as MASLD.

BACKGROUND

Idiosyncratic drug-induced liver injury, hereinafter referred to as DILI, is an adverse reaction to the use of prescription and over-the-counter medications, herbal products, and dietary supplements (1). DILI results from an abnormal and dysregulated overactivation of the innate and specific immune responses, and it is the most common cause of acute liver failure in Western countries (2). DILI is multifactorial and unpredictable, as its presentation results from a combination of host, pharmacological, and environmental factors (3). For this reason, DILI is considered a complex disease in which patients' unique genetic and epigenetic features determine, at least in part, their response to a given xenobiotic (4–7). The absence of specific diagnostic tests for DILI, combined with the difficulty of identifying susceptibility profiles, makes it a public health burden.

DILI susceptibility is the sum of genetic background and multiple environmental factors that regulate gene expression through epigenetic mechanisms, such as DNA methylation and non-coding RNAs (ncRNA) (8). DNA methylation alterations have been identified as a risk factor for antituberculosis drug-associated DILI (ATDILI) in Asian countries where tuberculosis has a high

prevalence (9–14). However, little is known about DILI epigenetics, and particularly about DNA methylation within this context. DNA methylation regulation is highly complex, entailing a multilevel network of biochemical reactions that encompasses metabolic processes and gene expression. In brief, DNA methylation occurs in CpG dinucleotides via DNA methyltransferases (DNMTs), which catalyse the transfer of a methyl group from S-adenosyl methionine methyl donor to a cytosine, yielding 5-methylcytosine (15). There are two groups of DNMTs, DNMT1 and DNMT3. The DNMT3a and DNMT3b subtypes are typically associated with *de novo* methylation, whilst DNMT1 is generally associated with maintenance methylation (16, 17). However, there is evidence that all cooperate in establishing the methylation patterns during embryogenesis and in onward maintenance (18, 19). DNA demethylation is a much more intricate process, and it can occur passively in a replication-dependent manner or in an active way, involving many mechanisms, such as ten-eleven translocations, DNA deamination and repair (20, 21). DNA methylation modulates gene expression in various biological processes, including embryonic development, genomic imprinting, X-chromosome inactivation, suppression of transposable elements, maintenance of genome stability and haematopoiesis regulation (22–26).

Environmental factors, such as toxic exposures, pharmaceuticals, diet, and psychosocial stress, influence disease onset and progression through DNA methylation modifications. Severe stress enhances global DNA methylation, as well as the expression of interleukin-6, DNMT1/3A/3B, and EZH2(27). Hydralazine, a very common hypertensive medication, has demethylating effects on DNA, leading to immunological diseases such as drug-induced lupus-like syndrome (28). Several studies suggested that diet might be associated with global and specific patterns of DNA methylation (29). Overall, healthy dietary habits have a positive influence on DNA methylation during ageing, increasing global methylation status (30).

This methylome-wide association study (MWAS) aims to identify DILI differential methylation signatures and gene modules with correlated DNA methylation patterns nearby the transcription start site (TSS), as well as to provide an initial insight into the biological processes affected by DNA methylation regulation in DILI.

METHODS

Study participants and study design

Thirty-two DILI patients included in the Spanish DILI Registry, recruited at the Virgen de la Victoria University Hospital and the Málaga University Regional Hospital, and 33 healthy controls, volunteers who underwent their yearly medical examination at the Occupational Medicine Unit of the Málaga University were analysed.

DILI patient inclusion criteria were as follows: a) Alanine aminotransferase ≥ 5× upper limit of normal (ULN) or alanine aminotransferase ≥ 3 ×ULN + total bilirubin > 2 ×ULN or alkaline phosphatase ≥ 2× ULN; b) chronological relationship consistent with exposure to the suspected agent and the onset of liver injury; c) exclusion of alternative causes of liver injury. Individuals under 18 years of age, patients or their legal representatives who were unable or unwilling to provide informed consent, and patients with other forms of acute liver damage were excluded.

Healthy controls had been under pharmacological treatment but were tolerant to the drugs, and their liver biochemical profile was normal. Exclusion criteria were persons aged less than 18 years, inability to provide written informed consent, and individuals with underlying liver disease or abnormal liver tests.

The study protocol, which conforms to the ethical guidelines outlined in the Declaration of Helsinki, was approved by the local Ethical Committee at the Virgen de la Victoria University Hospital, Málaga, Spain. All patients and controls signed informed consent before being included in the study.

Sample collection and DNA extraction

Venous whole blood samples from each DILI patient were collected in EDTA-anticoagulated tubes within one week of liver injury detection. All healthy controls blood samples were collected at the moment of inclusion in the study. The blood samples were stored at -80°C at the Provincial Biobank of Málaga-IBIMA, which is part of the Biobank of the Public Health System of Andalusia and the National Biobank Platform.

DNA extraction and microarray analysis

DNA was extracted from whole blood samples using the DNeasy Blood & Tissue Kit (QIAGEN, USA), and DNA bisulphite conversion was done using the EZ-96 DNA Methylation kit (Zymo Research, Irvine, CA). A methylome-wide screening analysis was conducted using the Infinium MethylationEPIC 850k BeadChip Kit (Illumina, San Diego, CA).

Methylome-wide analysis

The β-values density distribution revealed measurement errors in controls 65 and 21, which were subsequently eliminated in a first quality control stage. Methylation β-values were normalised for the type of probe using the Beta Mixture Quantile method with ChAMP (31). Sex and age covariate correction was performed with *limma* (32).

Differentially methylated positions (DMP) analysis was performed with *limma* (32), and age and sex covariates were included when fitting the linear model. False discovery rate (FDR) corrected p-values ≤ 0.05 were considered significant. DMP analysis power calculation yielded a mean power value of 0.83 for detecting significant hypomethylated CpG sites within the |Δβ| range of 0.05 to 0.17, and a mean power value of 0.54 for detecting significant hypermethylated CpG sites within the same size effect range. A χ^2 test was performed to assess whether the significant CpG sites distribution across genomic regions (first exon, 3'UTR, 5'UTR, body, exon intron boundary, intergenic region, TSS200, and TSS1500) was random, and a correlation plot of the standardised residues was obtained **(Figure S1).**

WGCNA-based DNA methylation analysis was performed with CWGCNA (33). CpG sites in the TSS1500, TSS200 and the first exon regions were included in the analysis, given the significant CpG sites distribution across genomic regions and the general rule that CpG sites near the TSS are involved in gene expression regulation.

Differentially methylated regions (DMRs) were identified with the *DMRcate* package (34), those with a harmonic mean of the individual CpG p-values (HMFDR) ≤ 0.05 were considered significant. Information about the genes associated with the top ten most significant differentially methylated CpG sites and regions was extracted from the Human Protein Atlas (HPA) (https://www.proteinatlas.org/), Gene Cards (https://www.genecards.org/), and OMIM (https://www.omim.org/) databases and UCSC Genome Browser (https://genome.ucsc.edu/).

A pathway enrichment analysis was performed for the significant differentially methylated gene modules using *enrichR* and *enrichplot* packages with the Canonical pathways and Gene Ontology (GO) collections for cellular component and biological process from the Human Molecular Signature Database Collections (https://www.gsea-msigdb.org/gsea/msigdb/collections.jsp) (35, 36). Additionally, a tissue enrichment analysis was done with TissueEnrich and the HPA database (37). Pathways with FDR ≤ 0.05 were considered significant. Methylation analyses were carried out with R software versions 4.3.3, 4.4.0, 4.4.2 and 4.5.0 (38). A representation of the overall MWAS workflow is shown in Fig. 1.

RESULTS

Patients characteristics

Initially, the study comprised 32 DILI patients and 33 healthy controls. Following methylation data quality control, all analyses were conducted on a cohort of 32 DILI patients and 31 healthy controls, with a median age of 53 years (38–67) and 54 years (38–61), respectively. The most common type of DILI was hepatocellular, and antibiotics were the most frequent causative group **(**Table 1**).**

Table 1
Demographics, clinical characteristics, and biochemical parameters of patients with idiosyncratic drug-induced liver injury and healthy controls

Age (years), median (IQR)	**DILI (n = 32)**	**Controls (n = 31)**
	53 (38–67)	**54 (38–61)**
Female sex, n (%)	12 (38)	17 (55)
Type of liver injury, n (%)		
Hepatocellular	17 (53)	NA
Cholestatic	10 (31)	NA
Mixed	5 (16)	NA
Culprit drug class, n (%)		
Antibiotics	17 (53)	NA
Dietary supplements	3 (9.4)	
Antineoplastic agents	2 (6.3)	
Antidepressants	1 (3.1)	
Antifungals	1 (3.1)	
Antispasmodics	1 (3.1)	
Antithyroid combinations	1 (3.1)	
Antivirals	1 (3.1)	
Corticosteroids	1 (3.1)	
Non-steroidal anti-inflammatory drugs	1 (3.1)	
Statins	1 (3.1)	
Laboratory parameters at DILI recognition, median (IQR)		
Alanine aminotransferase (IU/L)	267 (191–613)	25 (21–34)
Aspartate aminotransferase (IU/L)	183 (114–466)	26 (22–31)
Alkaline phosphatase (IU/L)	181,50 (101–261)	87 (50–120)
Total bilirubin (mg/dl)	4.2 (0.5–8.5)	0.7 (0.5–1.2)

IQR: interquartile ranges, NA: not applicable. Continuous variables are represented with median and interquartile ranges (Q1 and Q3), and categorical variables are expressed as percentages.

Methylome-wide association analysis in DILI

DMP analysis

A volcano plot of the total 599,555 analysed CpG probes showed that significant CpG positions in DILI patients were mostly hypomethylated in comparison with healthy controls, with a higher prevalence of CpG sites in the Δβ values < 0 region. DMP analysis revealed 52,253 significant CpG sites in DILI (FDR ≤ 0.05), with 12,505 hypermethylated (Δβ values > 0) and 39,748 hypomethylated (Δβ values < 0) **(**Fig. 2**).**

The ten most significant differentially methylated CpG positions in DILI patients were: cg10297007, cg17565444, cg26886885, cg15812586, cg04772795, cg14952878, cg05756439, cg10555744, cg21467365, and cg23691006 **(**Table 2**)**.

Table 2
Top ten significant CpG sites in DILI patients compared to healthy controls

CpG	Adjusted p-value (FDR)	Δβ	CHR	Position	Gene	Localisation
cg10297007	2.29×10^{-5}	-0.045	6	16699991	*ATXN1*	5'UTR-opensea
cg17565444	2.29×10^{-5}	-0.048	14	94429203	*ASB2*	Body-opensea
cg26886885	2.29×10^{-5}	-0.048	16	85603371		IGR-opensea
cg15812586	2.29×10^{-5}	-0.060	7	139953117		IGR-opensea
cg04772795	2.29×10^{-5}	-0.059	8	134228900	*WISP1*	Body-opensea
cg14952878	2.29×10^{-5}	0.075	17	37259084	*PLXDC1*	Body-opensea
cg05756439	2.31×10^{-5}	-0.038	6	88632781		IGR-opensea
cg10555744	2.31×10^{-5}	0.076	1	25946258	*MAN1C1*	Body-shore
cg21467365	2.31×10^{-5}	0.097	2	197039306		IGR-shelf
cg23691006	2.31×10^{-5}	-0.059	17	1510666	*SLC43A2*	Body-shore

FDR: false discovery rate, CHR: chromosome 5'UTR-opensea: 5' untranslated region-opensea, IGR-opensea: intergenic region-opensea, IGR-shelf: intergenic region-shelf.

Regarding the χ2 test, significant CpG sites were not distributed randomly across genomic regions (p-value < 2.2×10^{-16}), with significant hypomethylated CpG sites tending towards the TSS1500 and TSS200 regions, whilst significant hypermethylated CpG sites were mostly located in the gene body region **(Figure S1).**

DMR analysis

An analysis of the distribution of CpG site methylation hotspots in DILI revealed the top ten DMRs **(Figure S3).** The most significant hypomethylated region was DMR1 on chr 1:117046471–117047420 (HMFDR = 3.43×10^{-5}) within the body of *ENSG00000298543*, which codifies a long non-coding RNA (lncRNA) antisense to CD58 and IGSF3 mRNAs. Also, it is worth mentioning hypomethylated DMR6 on chr15: 55513621–55513770 (HMFDR = 4.97×10^{-5}), located in *RAB27A* body, a gene from the RAS oncogene family that regulates cytotoxic T-cell granule release. As well as hypomethylated DMR2 in chr17:17311855–17311867, for its location within a long-interspersed nuclear element type 1 (LINE-1) region **(**Table 3**).**

Table 3
Top ten significant DMRs in DILI patients

DMR	Localisation	Length	Mean methylation status	HMFDR	Transcript	Gene coordinates	Description
DMR1	chr1: 1170464711-17047420	949	Hypomethylated	3.43×10^{-5}	ENSG00000298543	Body (intron 1)	*ENSG00000298543* is an RNA gene affiliated with the lncRNA class. Antisense to CD58 and IGSF3
DMR2	chr17: 17311855–17311867	12	Hypomethylated	3.69×10^{-5}	Intergenic (LINE, L1MC4a)	NA	NA
DMR3	chr17: 73310148–73310222	74	Hypomethylated	3.96×10^{-5}	Intergenic	NA	NA
DMR4	chr5: 148185121–148185745	624	Hypomethylated	4.48×10^{-5}	Intergenic	NA	NA
DMR5	chr19: 39224370–39225148	778	Hypomethylated	4.77×10^{-5}	*CAPN12*	Body	The calpains, calcium-activated neutral proteases, are non-lysosomal, intracellular cysteine proteases. The mammalian calpains include ubiquitous, stomach-specific, and muscle-specific proteins
DMR6	chr15: 55513621–55513770	149	Hypomethylated	4.97×10^{-5}	*RAB27A*	Body	*RAB27A* (RAB27A, Member RAS Oncogene Family) is a protein-coding gene. It regulates the homeostasis of the late endocytic pathway, including endosomal positioning, maturation and secretion, also it plays a role in cytotoxic granule exocytosis in lymphocytes. *RAB27A* deficiency is responsible for Griscelli syndrome type II
DMR7	chr7: 139952594–139953118	524	Hypomethylated	5.03×10^{-5}	ENSG00000307329	Body	ENSG00000307329 is an RNA gene affiliated with the lncRNA class
DMR8	chr16: 85603371–85604048	677	Hypomethylated	5.27×10^{-5}	Intergenic	NA	NA

DMRs: differentially methylated region, CHR: chromosome, NA: not available, HMFDR: harmonic mean false discovery rate, LINE: long interspersed element type 1, RNA: ribonucleic acid, lncRNA: long non-coding RNA, IGSF3: immunoglobulin superfamily member 3, MITF-M: melanocyte-inducing transcription factor, NA: not applicable.

DMR	Localisation	Length	Mean methylation status	HMFDR	Transcript	Gene coordinates	Description
DMR9	chr15: 67200651–67200880	229	Hypomethylated	5.31×10^{-5}	Intergenic (LINE, L2b)	NA	NA
DMR10	chr19: 2168535–2169161	626	Hypomethylated	5.31×10^{-5}	*DOT1L*	Body	The protein encoded by this gene is a histone methyltransferase that methylates lysine-79 of histone H3

DMRs: differentially methylated region, CHR: chromosome, NA: not available, HMFDR: harmonic mean false discovery rate, LINE: long interspersed element type 1, RNA: ribonucleic acid, lncRNA: long non-coding RNA, IGSF3: immunoglobulin superfamily member 3, MITF-M: melanocyte-inducing transcription factor, NA: not applicable.

Table 3. Top ten significant DMRs in DILI patients (*Table 3 is in the "Tables" section at the end of the document)

WGCNA-based DNA methylation profiling analysis

DILI WGCNA-based methylation analysis revealed two differential methylation modules with significant eigengenes, module 0 (ME0) and module 1 (ME1). ME0 comprised 1,217 genes, while ME1 had 3,423 genes with significant mean differential methylation values for the TSS1500, TSS200 and the first exon regions as a whole (FDR = 7.13×10^{-5} and FDR = 1.29×10^{-10}, respectively) (Fig. 3A). ME1 volcano plot revealed 1,219 significant differentially hypermethylated genes and 1,731 hypomethylated genes (FDR ≤ 0.05), and 473 genes with non-significant differential methylation between DILI and controls. The most significant differentially hypomethylated genes in ME1 were *SLFN12*, *CD244*, *ANKRD53*, *RNF19A* and *EVPLL*, while the most significant differentially hypermethylated genes were *MIR342*, *MPHOSPH9*, *TXK*, *MIR4751* and *LOC101927166* (Fig. 3B). In contrast, the ME0 volcano plot revealed 49 significant hypermethylated genes and 142 hypomethylated genes (FDR ≤ 0.05), and 1,026 genes with non-significant differential methylation in DILI compared with controls. The most differentially hypomethylated genes in ME0 were *SNORD7*, *LOC283299*, *CSRNP3*, *LOC101928414*, *LINC01115*, whilst the most differentially hypermethylated genes in ME0 were *LINC01312*, *PIWIL1*, *LIPN*, *HRASLS*, and *LOC101927636* (Fig. 3C).

WGCNA-based DNA methylation tissue enrichment analysis

ME0 differentially methylated protein-coding genes tissue enrichment analysis bar plot showed that the most enriched tissues in DILI patients were the testis, the liver, the salivary glands and the tonsils (Fig. 4A). Regarding ME0, the most enriched tissues were the bone marrow, the liver and the skin (Fig. 4B).

WGCNA-based DNA methylation functional enrichment analysis

ME0 differentially methylated genes functional enrichment analysis with the Canonical pathways database revealed that the most significant pathway associated with ME0 genes was "Kegg olfactory transduction" followed by "Kegg olfactory signaling pathways" and "Kegg keratinization" (Fig. 5A). ME1 Canonical pathways dot plot showed that the most significant pathways associated with ME1 genes were "Kegg olfactory signaling pathway", "Kegg olfactory transduction" and "Kegg neutrophil degranulation" (Fig. 5B).

ME0 GO biological process functional enrichment analysis most significant pathways were "Sensory perception of chemical stimulus", "Detection of stimulus involved in sensory perception", and "Sensory perception of smell"(Fig. 6A). Meanwhile, in ME1 the main GO biological process pathways were "Sensory perception of chemical stimulus", "Detection of stimulus involved in sensory perception", "Sensory perception of smell", and "Adaptive immune system response" (Fig. 6B).

ME1 GO cellular component analysis most significant pathways were "External side of plasma membrane", "Collagen containing extracellular matrix", and "Vesicle lumen". Conversely, ME0 GO cellular component functional enrichment analysis did not reveal any significant pathway (Fig. 7).

DISCUSSION

DILI epigenetics are poorly understood, with most studies focusing on DNA methylation alterations in ATDILI (8). Our results showed an aberrant global hypomethylation in DILI patients in comparison with healthy controls, which could lead to genomic instability, promoting disease onset and progression (39, 40). Moreover, hypomethylated DMR2 was localised within a long-interspersed nuclear element 1 (LINE-1) region. Previous evidence has shown LINE-1 hypomethylation as an ATDILI risk factor (9), as well as a predictor of a broad range of diseases (41, 42), due to LINE-1 hypomethylation association with general genomic instability and disease onset.

The most significant DNA methylation hotspot in DILI was DMR1, a hypomethylated region located in the body of the gene *ENSG00000298543*, which encodes for a lncRNA antisense to CD58 and IGSF3. CD58 is a CD8 + T-cell costimulatory receptor, whereas IGSF3 activates NF-kβ in hepatocellular carcinoma (HCC) (43–45). CD8 + T-cells are known as the most abundant leukocytes in DILI and the main responsible for hepatocyte death. Another DMR worth mentioning is hypomethylated DMR6, which is colocalised within the body of *RAB27A*, a gene that transcribes for a protein from the *RAS* oncogene family involved in the homeostasis of the late endocytic pathway. *RAB27A* deficiency is associated with Griscelli syndrome type II (GSII), an autosomal recessive disease in which disrupted cytotoxic granule release results in a defective immune response with excessive activation of macrophages. GSII often leads to haemophagocytic lymphohistiocytosis, a life-threatening immunological disorder characterised by the release of inflammatory cytokines coupled with cytopenia, which results in hyperinflammation and hepatosplenomegaly (46, 47). As a general rule, hypomethylation within the gene body indicates gene transcription downregulation (48, 49). Consequently, differential methylation of DMR1 and DMR6 in DILI could regulate gene transcription, thereby enhancing the overactivation of cytotoxic CD8 + T-cells with aberrant degranulation, ultimately leading to hepatocyte death. Hypomethylated DMR10 in the *DOT1L* gene body is also interesting, as DNA methylation landscape is moulded by other epigenetic mechanisms as well. *DOT1L* encodes a unique histone methyltransferase that methylates the lysine-79 of histone H3 (H3K79), which is known as an active transcription mark in mammalian genes involved in RNA polymerase II transcription, DNA damage response and cell cycle checkpoint activation (50). Likewise, *in vitro* studies with CD8 + T-cells have shown that *DOT1L* downregulation leads to an impaired T-cell immune response through H3K79me2 demethylation (51). All this showcases the interplay of multifaceted and dynamic mechanisms behind DILI pathophysiological processes.

Regarding WGCNA-methylation-based gene modules, two significant gene modules, ME0 and ME1, with highly correlated DNA methylation levels and distinct protein-coding gene tissue methylation profiles were revealed in DILI patients' whole blood samples. This indicates not only two clusters of co-methylated functionally related genes, but also two possible gene expression patterns in DILI, as nearby TSS methylation status typically correlates with gene expression (49). Furthermore, in the protein-coding gene tissue enrichment analysis, the results suggest the presence of circulating cell-free DNA from tissue-specific and tissue-enriched protein-coding genes released by a variety of tissues in DILI whole blood samples. This is important since, for the most part, whole blood extracted DNA usually comes from leukocytes, which makes it difficult to detect DNA methylation signatures from origin other than white blood cells in whole blood samples. ME1 included protein-coding genes whose expression was mostly enriched in the bone marrow, the liver, and the skin, as expected in DILI, in which the immune system activation is a key determinant, as well as the liver injury-associated processes. ME0 protein-coding genes were mainly enriched in the testis, but also in the liver, the salivary glands and the tonsils. This could be explained by sex-related differences in DILI pathophysiology, as although sex covariate correction was performed on the methylation data, there could be underlying differences causing the appearance of ME0, which is a module for male-associated DILI. Previous studies have reported the existence of sexual dimorphism in the immune response, and more specifically, the influence of sex hormones on hepatic metabolism and immune mechanisms, as well as differences in the response to oxidative stress and liver regeneration between females and males, which altogether could influence the presentation of DILI (52–54).

In relation to the totality of ME1 genes, it is worth noting *MIR342* hypermethylation in the TSS vicinity, and its possible downregulation in DILI. *MIR342* has also been found to be downregulated in metabolic dysfunction-associated steatotic liver disease (MASLD) and metabolic dysfunction-associated steatohepatitis (MASH). This is relevant as accumulating evidence has shown that idiosyncratic DILI induced by specific drugs shares pathophysiological processes with MASLD, with obesity as a possible common risk factor (55, 56). Additionally, miR-342 has been shown to target the wnt/β-catenin and NF-kβ pathways in HCC cells (57, 58). Hence, *MIR342* differential methylation could regulate both immune processes and apoptotic mechanisms in a

broad spectrum of liver diseases, including DILI. In the context of autoimmune inflammation in the central nervous system and allergic airway inflammation in the lung, *MIR342* deficiency has been associated with metabolic dysfunction of regulatory T-cells, which could influence the immunoregulatory functions of these cells, enhancing inflammation and autoimmune reactions (59). Not only *MIR342* hypermethylation is of great interest, but also hypomethylated *CD244*, for its role in the activation of T cytotoxic cells and natural killer cells (60), correlating with the impaired immune response overactivation observed in DILI. On the other hand, regarding the overall ME0 gene content, the most significant genes were mostly lncRNAs and many yet to be functionally characterised *loci*. For instance, hypomethylated *LOC283299* is predicted to encode a lncRNA antisense to *OR5E1P*, which is a gene predicted to transcribe for an olfactory receptor.

Regarding functional analysis, ME1 and ME0 Canonical pathways dot plots showed that the most enriched term was “Kegg olfactory signaling pathway”, followed by “Kegg olfactory transduction”. This finding aligns with what was previously discussed regarding *LOC283299* function. Hepatocyte olfactory receptors (ORs) sense the metabolic status of the body and participate in hepatic homeostasis. In fact, *in vitro* studies have shown an association between ORs and lipid metabolism in hepatocytes (61, 62), with evidence supporting a link between OR gene variants and extreme obesity with progression to MASH (63). Furthermore, a previous study on systems pharmacology with networks of drugs clustered according to their protein targets has shown the association between pharmacological drugs with hepatotoxic potential and ORs, indicating their relevance in DILI liver damage signalling pathways (64). Our functional annotation analyses also indicated the implication of DNA methylation dysregulation behind DILI immune impairment. The neutrophil-associated innate immune response and the activation of the adaptive immune system were demonstrated to be key processes, as well as the endocytic secretory granule pathway, as also indicated by DMR1 and DMR6. However, these phenotypes are shared with other liver diseases such as MASLD (65).

The present MWAS could be considered a preliminary study, as it was conducted on a heterogeneous DILI cohort characterised by a variety of culprit hepatotoxicant agents and a modest sample size, in order to provide a first insight into the pathophysiological mechanisms affected by DNA methylation modifications in DILI. The identification of tissue-specific and tissue-enriched protein-coding gene differential methylation in blood from DILI patients could set the ground for DNA methylation-based biomarker research in DILI. However, a group with liver diseases other than DILI would be needed to state whether these DNA methylation signatures are DILI-specific or not. Moreover, a growing body of evidence indicates the presence of common DNA methylation alterations in MASLD, viral hepatitis and HCC (66, 67), as their presentation and progression are influenced by shared environmental factors and comorbidities (68, 69). Here, our study of DILI patients’ methylome has also revealed possible DNA methylation similarities with other liver diseases, such as MASLD and HCC, which could provide a baseline for DILI susceptibility screening studies that take in count the presence of other underlying liver diseases, both in progression with evident manifestations and at very early stages without clinical manifestations. However, it is difficult to determine if the observed DNA methylation alterations in this study were present before DILI onset or acquired during the episode. Therefore, further analysis would be needed to determine susceptibility profiles associated with DILI and other liver diseases. Additionally, there is a need for gene expression analysis to bridge epigenetic regulation and gene transcription to confirm if the identified DNA methylation modifications affect gene expression patterns in DILI. Finally, regarding the power analysis results, mean statistical power for hypermethylated CpG sites is low given the fact that our sample size is reduced. Conversely, statistical power for hypomethylated CpG sites is great. Also, it is important to mention that we used limma ebayes linear regression method to detect differentially methylated positions, which tends to yield less significant CpG sites than other commonly used statistical tests for differential methylation assessment, such as Wilcoxon.

CONCLUSIONS

This study on DILI methylation landscape revealed an overall global hypomethylation, showing genomic instability as an influencing factor behind DILI. The most significant differential methylation hotspot in DILI was a hypomethylated region in *ENSG00000298543*, which could increase the immune system activation in DILI. Methylation-based WGCNA analysis revealed ME1 as the main gene methylation pattern in DILI, and ME0 as a secondary male-specific gene methylation module. Our analyses suggest the involvement of DNA methylation alterations not only in the exaggerated immune response activation in DILI but also in sensory receptor signalling pathways associated with it, as well as the interaction between DNA methylation and ncRNAs. Additionally, our analyses indicate possible shared epigenetic features with other liver diseases, such as MASLD.

Abbreviations

DILI
drug-induced liver injury
MASLD
metabolic dysfunction steatotic liver disease
ncRNA: non-coding RNA,MWAS
methylome-wide association study
DMP
differentially methylated positions
DMR
differentially methylated regions
WGCNA
weighted gene correlation network analysis
ME0
module 0
ME1
module 1
lncRNA
long non-coding RNA
ATDILI
antituberculosis drug-associated DILI
DNMT
DNA methyltransferase
TSS
transcription start site
HPA
Human Protein Atlas
HMFDR
harmonic mean of false discovery ratio
LINE
long-interspersed nuclear elements
HCC: hepatocellular carcinoma,GSII
Griscellis syndrome
H3K79
lysine-79 of histone H3
MASH
metabolic dysfunction-associated steatohepatitis
OR
olfactory receptors.

Declarations

ACKNOWLEDGEMENTS

Not applicable.

AUTHOR CONTRIBUTIONS

RLDLSF: conceptualisation, bioinformatic analyses (power analysis calculations, methylation data covariant correction and quality control, DMP, DMR, WGCNA, functional and tissue enrichment analysis), manuscript writing. GPL: conceptualisation, bioinformatic analysis (methylation data quality control). HN: study design, conceptualisation, manuscript critical revision. IAA: study design,

conceptualisation, manuscript critical revision. IDA: manuscript critical revision. JSC: manuscript critical revision. MVP: sample manipulation. AGJ: conceptualisation, manuscript critical revision. CS: conceptualisation, manuscript critical revision. LMI: conceptualisation, manuscript critical revision. IMC: conceptualisation, manuscript critical revision. RA: conceptualisation, manuscript critical revision. All authors have revised and approved the final version of the manuscript.

FUNDING

This study was funded by grants of Instituto de Salud Carlos III (ISCIII), cofounded by Fondo Europeo de Desarrollo Regional – FEDER, cofounded by European Union (grant number PI25/01205, PID2022-140169OB-C21, PT23/00137), by the Consejería de Salud y Familias, Junta de Andalucía (PI-0310-2018, PPRO-CTS649-G-2023, PPRO-CTS1032-G-2023), and by the Agencia Española de Medicamentos y Productos Sanitarios. CIBERehd and Plataforma de Investigación Clinica are funded by ISCIII. RLDLSF holds a PFIS contract funded by ISCIII (COD.SIA 991386). IAA holds a Miguel Servet contract funded by ISCIII (CP25/00033). JSC holds "Acción B-clinical research contract" from Junta de Andalucía (C1.2-0001-2025). IDA holds a Río Hortega contract funded by ISCIII (CM23/00103).

Ethics approval and consent to participate

The research was conducted in accordance with the Helsinki declaration and was approved by the local Ethical Committee at the Virgen de la Victoria University Hospital, Málaga, Spain.

Competing interests

The authors declare that they have no conflict of interest.

Consent for publication

Not applicable.

References

1. Garcia-Cortes M, Robles-Diaz M, Stephens C, Ortega-Alonso A, Lucena MI, Andrade RJ. Drug induced liver injury: an update. Arch Toxicol. 2020;94(10):3381–407.
2. Reuben A, Koch DG, Lee WM. Drug-induced acute liver failure: results of a U.S. multicenter, prospective study. Hepatology. 2010;52(6):2065–76.
3. Chen M, Suzuki A, Borlak J, Andrade RJ, Lucena MI. Drug-induced liver injury: Interactions between drug properties and host factors. J Hepatol. 2015;63(2):503–14.
4. Lucena MI, Molokhia M, Shen Y, Urban TJ, Aithal GP, Andrade RJ, et al. Susceptibility to amoxicillin-clavulanate-induced liver injury is influenced by multiple HLA class I and II alleles. Gastroenterology. 2011;141(1):338–47.
5. Cirulli ET, Nicoletti P, Abramson K, Andrade RJ, Bjornsson ES, Chalasani N, et al. A Missense Variant in PTPN22 is a Risk Factor for Drug-induced Liver Injury. Gastroenterology. 2019;156(6):1707–e17162.
6. Singh S, Kumar PK, Kumar JP, Tomo S, Yadav D, Sharma P, et al. Genetic and epigenetic basis of drug-induced liver injury. In Thieme Medical Publishers, Inc.; 2023. pp. 163–75.
7. Stephens C, Andrade RJ. Genetic predisposition to drug-induced liver injury. Clin Liver Dis. 2020;24(1):11–23.
8. de Los Santos-Fernández RL, Segovia-Zafra A, Paz-López G, Matilla-Cabello G, Niu H, Álvarez-Álvarez I, et al. Epigenetic modifications in drug-induced liver injury: A systematic review. Br J Clin Pharmacol. 2025;91(6):1660–74.
9. Udomsinprasert W, Sakuntasri W, Jittikoon J, Chaikledkaew U, Honsawek S, Chantratita W, et al. Global DNA hypomethylation of Alu and LINE-1 transposable elements as an epigenetic biomarker of anti-tuberculosis drug-induced liver injury. Emerg Microbes Infect. 2021;10(1):1862–72.
10. Zhang D, Hao J, Hou R, Yu Y, Hu B, Wei L. The role of NAT2 polymorphism and methylation in anti-tuberculosis drug-induced liver injury in Mongolian tuberculosis patients. J Clin Pharm Ther. 2019;45(3):561–9.

11. Huai C, Wei Y, Li M, Zhang X, Wu H, Qiu X, et al. Genome-Wide Analysis of DNA Methylation and Antituberculosis Drug-Induced Liver Injury in the Han Chinese Population. Clin Pharmacol Ther. 2019;106(6):1389–97.
12. Zhang J, Zhu X, Li Y, Zhu L, Li S, Zheng G, et al. Correlation of CpG island methylation of the cytochrome P450 2E1/2D6 genes with liver injury induced by anti-tuberculosis drugs: a nested case-control study. Int J Environ Res Public Health. 2016;13(8):776.
13. He L, Gao L, Shi Z, Li Y, Zhu L, Li S, et al. Involvement of cytochrome P450 1A1 and glutathione S-transferase P1 polymorphisms and promoter hypermethylation in the progression of anti-tuberculosis drug-induced liver injury: a case-control study. PLoS ONE. 2015;10(3):e0119481.
14. Chong Y, Zhu H, Ren Q, Ma X, Feng F. Interaction between the HIF-1α gene rs1957757 polymorphism and CpG island methylation in the promoter region is associated with the risk of anti-tuberculosis drug-induced liver injury in humans: A case–control study. J Clin Pharm Ther. 2022;47(7):948–55.
15. Moore LD, Le T, Fan G. DNA methylation and its basic function. Neuropsychopharmacology. 2013;38(1):23–38.
16. Jones PA. Functions of DNA methylation: islands, start sites, gene bodies and beyond. Nat Rev Genet. 2012;13(7):484–92.
17. Tajima S, Suetake I, Takeshita K, Nakagawa A, Kimura H. Domain Structure of the Dnmt1, Dnmt3a, and Dnmt3b DNA Methyltransferases. Adv Exp Med Biol. 2016;945:63–86.
18. Liang G, Chan MF, Tomigahara Y, Tsai YC, Gonzales FA, Li E, et al. Cooperativity between DNA methyltransferases in the maintenance methylation of repetitive elements. Mol Cell Biol. 2002;22(2):480–91.
19. Kim G, Ni J, Kelesoglu N, Roberts RJ, Pradhan S. Co-operation and communication between the human maintenance and de novo DNA (cytosine-5) methyltransferases. The EMBO J.; 2002.
20. Bochtler M, Kolano A, Xu GL. DNA demethylation pathways: Additional players and regulators. BioEssays. 2017;39(1):1–13.
21. Prasad R, Yen TJ, Bellacosa A, Active. DNA demethylation-The epigenetic gatekeeper of development, immunity, and cancer. Adv Genet (Hoboken). 2021;2(1):e10033.
22. Smith ZD, Meissner A. DNA methylation: roles in mammalian development. Nat Rev Genet. 2013;14(3):204–20.
23. Meng H, Cao Y, Qin J, Song X, Zhang Q, Shi Y, et al. DNA methylation, its mediators and genome integrity. Int J Biol Sci. 2015;11(5):604–17.
24. Bourc'his D, Bestor TH. Meiotic catastrophe and retrotransposon reactivation in male germ cells lacking Dnmt3L. Nature. 2004;431(7004):96–9.
25. Chang SC, Tucker T, Thorogood NP, Brown CJ. Mechanisms of X-chromosome inactivation. Front Biosci. 2006;11:852–66.
26. Álvarez-Errico D, Vento-Tormo R, Sieweke M, Ballestar E. Epigenetic control of myeloid cell differentiation, identity and function. Nat Rev Immunol. 2015;15(1):7–17.
27. Murphy TM, O'Donovan A, Mullins N, O'Farrelly C, McCann A, Malone K. Anxiety is associated with higher levels of global DNA methylation and altered expression of epigenetic and interleukin-6 genes. Psychiatr Genet. 2015;25(2):71–8.
28. Arce C, Segura-Pacheco B, Perez-Cardenas E, Taja-Chayeb L, Candelaria M, Dueñnas-Gonzalez A. Hydralazine target: from blood vessels to the epigenome. J Transl Med. 2006;4:10.
29. Maugeri A, Barchitta M. How Dietary Factors Affect DNA Methylation: Lesson from Epidemiological Studies. Med (Kaunas). 2020;56(8).
30. García-García I, Grisotto G, Heini A, Gibertoni S, Nusslé S, Gonseth Nusslé S, et al. Examining nutrition strategies to influence DNA methylation and epigenetic clocks: a systematic review of clinical trials. Front Aging. 2024;5:1417625.
31. Morris TJ, Butcher LM, Feber A, Teschendorff AE, Chakravarthy AR, Wojdacz TK, et al. ChAMP: 450k chip analysis methylation pipeline. Bioinformatics. 2014;30(3):428–30.
32. Ritchie ME, Phipson B, Wu D, Hu Y, Law CW, Shi W, et al. limma powers differential expression analyses for RNA-sequencing and microarray studies. Nucleic Acids Res. 2015;43(7):e47–47.
33. Liu Y. CWGCNA: an R package to perform causal inference from the WGCNA framework. NAR Genom Bioinform. 2024;6(2):lqae042.
34. Peters TJ, Meyer B, Ryan L, Achinger-Kawecka J, Song J, Campbell EM, et al. Characterisation and reproducibility of the HumanMethylationEPIC v2.0 BeadChip for DNA methylation profiling. BMC Genomics. 2024;25(1):251.

35. Jawaid W. enrichR: Provides an R Interface to 'Enrichr'. 2025.
36. Yu G, Hu E, Gao CH. enrichplot: Visualization of Functional Enrichment.
37. Jain A, Tuteja G, TissueEnrich. Tissue-specific gene enrichment analysis. Bioinformatics. 2019;35(11):1966–7.
38. R Core Team. R: A language and environment for statistical computing. Vienna, Austria; 2025.
39. Robertson KD. DNA methylation and human disease. Nat Rev Genet. 2005;6(8):597–610.
40. Zhang C, Sheng Q, Zhao N, Huang S, Zhao Y. DNA hypomethylation mediates immune response in pan-cancer. Epigenetics. 2023;18(1):2192894.
41. Park MK, Lee JC, Lee JW, Hwang SJ. Alu cell-free DNA concentration, Alu index, and LINE-1 hypomethylation as a cancer predictor. Clin Biochem. 2021;94:67–73.
42. Katsanou A, Kostoulas C, Liberopoulos E, Tsatsoulis A, Georgiou I, Tigas S. Retrotransposons Diabetes Mellitus Epigenomes. 2024;8(3).
43. Leitner J, Herndler-Brandstetter D, Zlabinger GJ, Grubeck-Loebenstein B, Steinberger P. CD58/CD2 Is the Primary Costimulatory Pathway in Human CD28-CD8 + T Cells. J Immunol. 2015;195(2):477–87.
44. Li B, Lu Y, Zhong MC, Qian J, Li R, Davidson D, et al. Cis interactions between CD2 and its ligands on T cells are required for T cell activation. Sci Immunol. 2022;7(74):eabn6373.
45. Sheng P, Zhu H, Zhang W, Xu Y, Peng W, Sun J, et al. The immunoglobulin superfamily member 3 (IGSF3) promotes hepatocellular carcinoma progression through activation of the NF-κB pathway. Ann Transl Med. 2020;8(6):378.
46. Maimaris J, Roa-Bautista A, Sohail M, Booth C, Cugno C, Chenchara L, et al. Griscelli Syndrome Type 2: Comprehensive Analysis of 149 New and Previously Described Patients with RAB27A Deficiency. J Clin Immunol. 2024;45(1):50.
47. Castaño-Jaramillo LM, Lugo-Reyes SO, Cruz Muñoz ME, Scheffler-Mendoza SC, Duran McKinster C, Yamazaki-Nakashimada MA, et al. Diagnostic and therapeutic caveats in Griscelli syndrome. Scand J Immunol. 2021;93(6):e13034.
48. Rountree MR, Bachman KE, Herman JG, Baylin SB. DNA methylation, chromatin inheritance, and cancer. Oncogene. 2001;20(24):3156–65.
49. Saxonov S, Berg P, Brutlag DL. A genome-wide analysis of CpG dinucleotides in the human genome distinguishes two distinct classes of promoters.PNAS. 2006;103(5):1412–7.
50. Wood K, Tellier M, Murphy S. DOT1L and H3K79 Methylation in Transcription and Genomic Stability. Biomolecules. 2018;8(1).
51. Bian Y, Li W, Kremer DM, Sajjakulnukit P, Li S, Crespo J, et al. Cancer SLC43A2 alters T cell methionine metabolism and histone methylation. Nature. 2020;585(7824):277–82.
52. Floreani A, Bizzaro D, Shalaby S, Taliani G, Burra P. Sex disparity and drug-induced liver injury. Dig Liver Dis. 2023;55(1):21–8.
53. Sutti S, Tacke F. Liver inflammation and regeneration in drug-induced liver injury: sex matters! Clin Sci (Lond). 2018;132(5):609–13.
54. Amacher DE. Female gender as a susceptibility factor for drug-induced liver injury. Hum Exp Toxicol. 2014;33(9):928–39.
55. Bessone F, Dirchwolf M, Rodil MA, Razori MV, Roma MG. Review article: drug-induced liver injury in the context of nonalcoholic fatty liver disease - a physiopathological and clinical integrated view. Aliment Pharmacol Ther. 2018;48(9):892–913.
56. Li X, Gao P, Niu J. Metabolic Comorbidities and Risk of Development and Severity of Drug-Induced Liver Injury. Biomed Res Int. 2019;2019:8764093.
57. Lu C, Jia S, Zhao S, Shao X. MiR-342 regulates cell proliferation and apoptosis in hepatocellular carcinoma through Wnt/β-catenin signaling pathway. Cancer Biomark. 2019;25(1):115–26.
58. Zhao L, Zhang Y. miR-342-3p affects hepatocellular carcinoma cell proliferation via regulating NF-κB pathway. Biochem Biophys Res Commun. 2015;457(3):370–7.
59. Yu R, Kim S, Li S, Yang W, Kim G, Lu LF, et al. Intronic miR-342 is a key regulator of cellular glycolysis in Foxp3 + regulatory CD4 T cells. J Immunol. 2025;214(11):2976–86.
60. Agresta L, Hoebe KH, Janssen EM. The emerging role of CD244 signaling in immune cells of the tumor microenvironment. Front Immunol. 2018;9:2809.
61. Wu C, Jia Y, Lee JH, Kim Y, Sekharan S, Batista VS, et al. Activation of OR1A1 suppresses PPAR-γ expression by inducing HES-1 in cultured hepatocytes. Int J Biochem Cell Biol. 2015;64:75–80.

62. Tong T, Ryu SE, Min Y, de March CA, Bushdid C, Golebiowski J, et al. Olfactory receptor 10J5 responding to α-cedrene regulates hepatic steatosis via the cAMP-PKA pathway. Sci Rep. 2017;7(1):9471.
63. Torres-Reyes LA, Gonzalez-Aldaco K, Panduro A, Jose-Abrego A, Roman S. Whole-Exome Sequencing identified Olfactory Receptor genes as a key contributor to extreme obesity with progression to nonalcoholic steatohepatitis in Mexican patients: Olfactory receptor genes in obese NASH patients. Ann Hepatol. 2022;27(6):100767.
64. Moya-García AA, González-Jiménez A, Moreno F, Stephens C, Lucena MI, Ranea JAG. Identification of New Toxicity Mechanisms in Drug-Induced Liver Injury through Systems Pharmacology. Genes (Basel). 2022;13(7).
65. Huang C, Fan X, Shen Y, Shen M, Yang L. Neutrophil subsets in noncancer liver diseases: Cellular crosstalk and therapeutic targets. Eur J Immunol. 2023;53(9):e2250324.
66. Kurokawa S, Yoneda M, Ogawa Y, Honda Y, Kessoku T, Imajo K, et al. Two differentially methylated region networks in nonalcoholic fatty liver disease, viral hepatitis, and hepatocellular carcinoma. BMC Gastroenterol. 2022;22(1):278.
67. Kim M, Delgado E, Ko S. DNA methylation in cell plasticity and malignant transformation in liver diseases. Pharmacol Ther. 2023;241:108334.
68. Huang SC, Liu CJ. Chronic hepatitis B with concurrent metabolic dysfunction-associated fatty liver disease: Challenges and perspectives. Clin Mol Hepatol. 2023;29(2):320–31.
69. Liu CJ, Seto WK, Yu ML. Dual-etiology MAFLD: the interactions between viral hepatitis B, viral hepatitis C, alcohol, and MAFLD. Hepatol Int. 2024;18(Suppl 2):897–908.

Figures

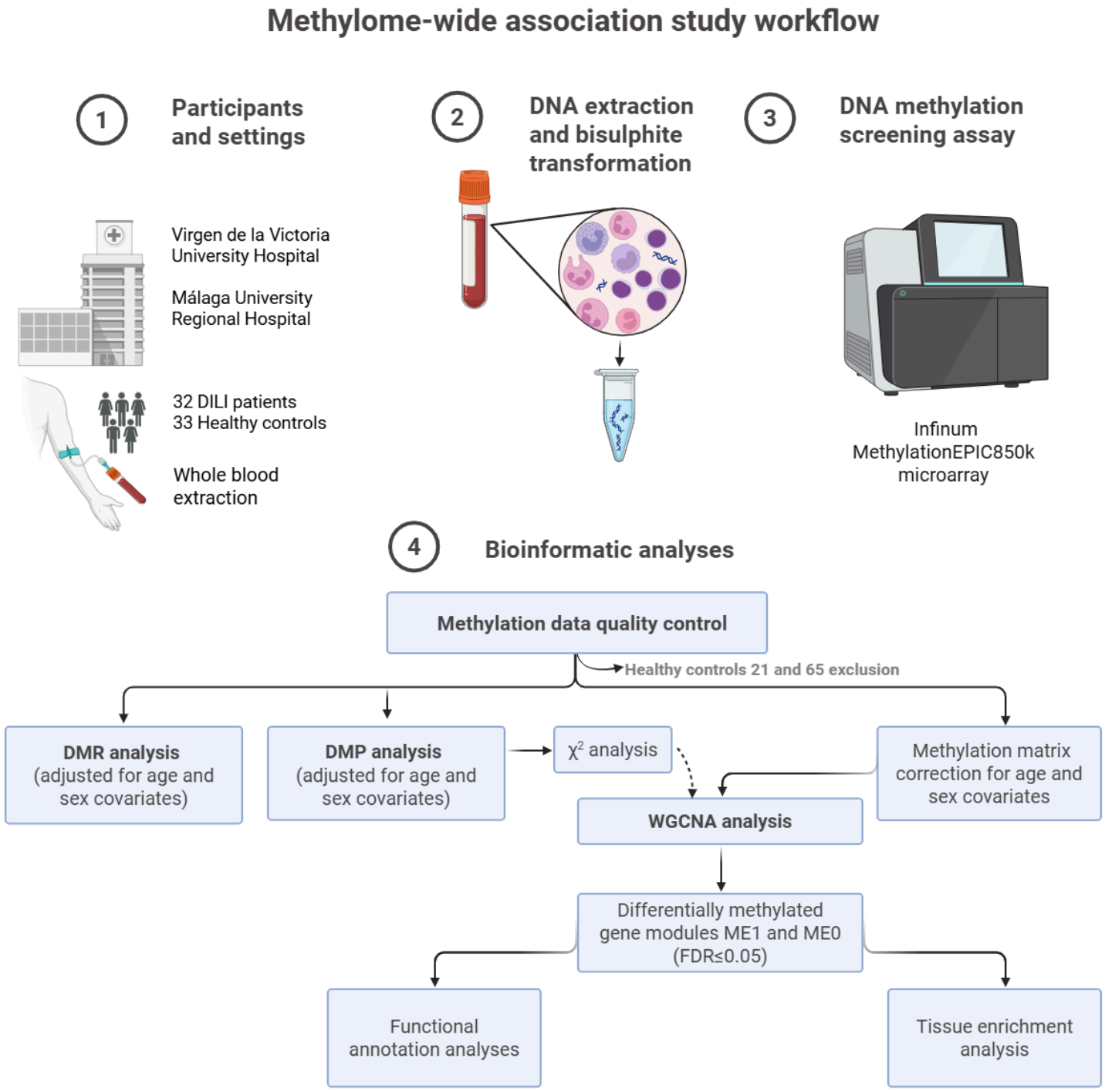


Figure 1

Workflow representation of the MWAS in DILI. Abbreviations: DMR: differentially methylated region, DMP: differentially methylated position, WGCNA: weighted gene correlation network analysis

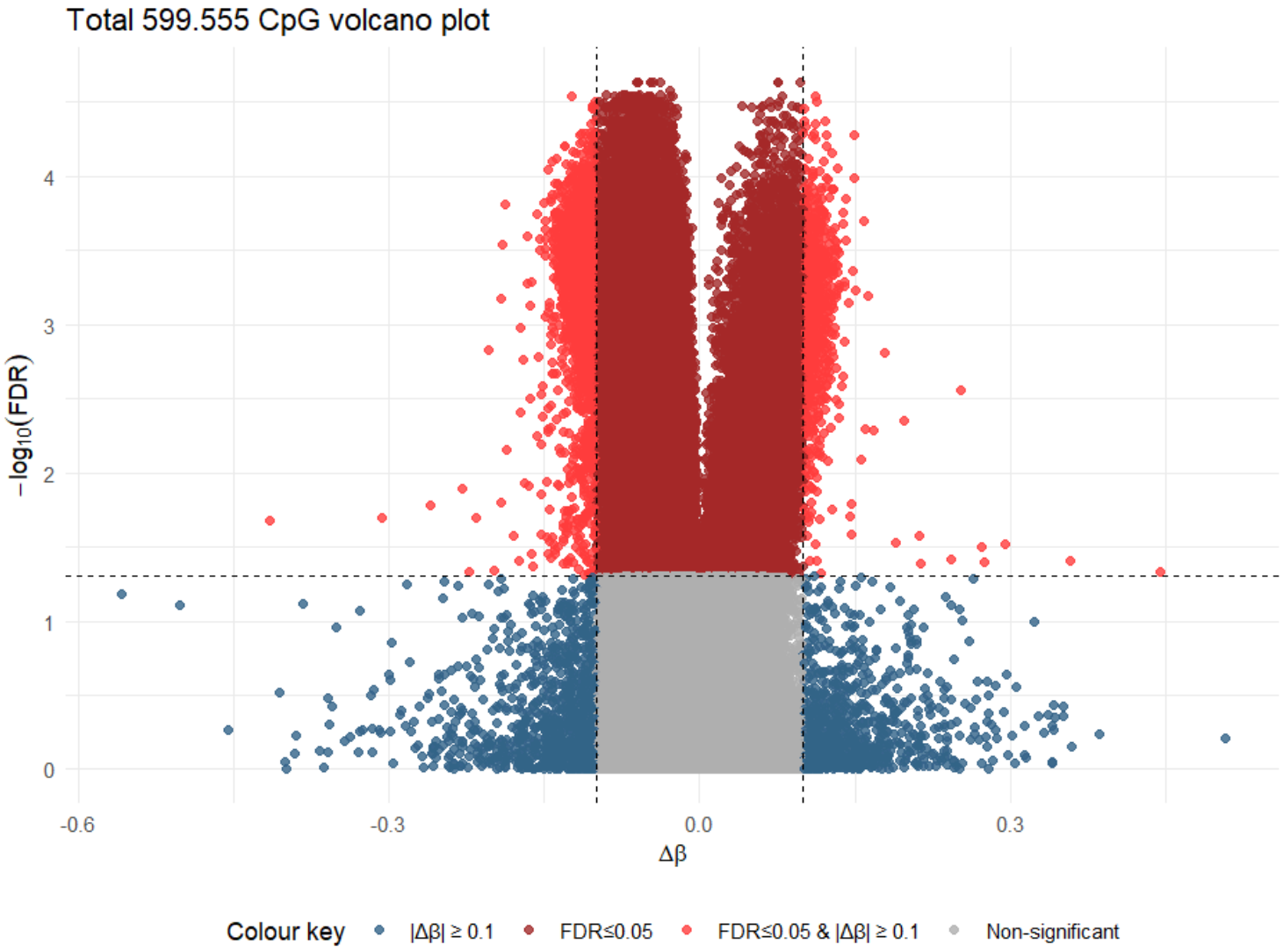


Figure 2

Volcano plot representation of the total analysed 599.555 CpG.Abbreviations: FDR: false discovery rate.

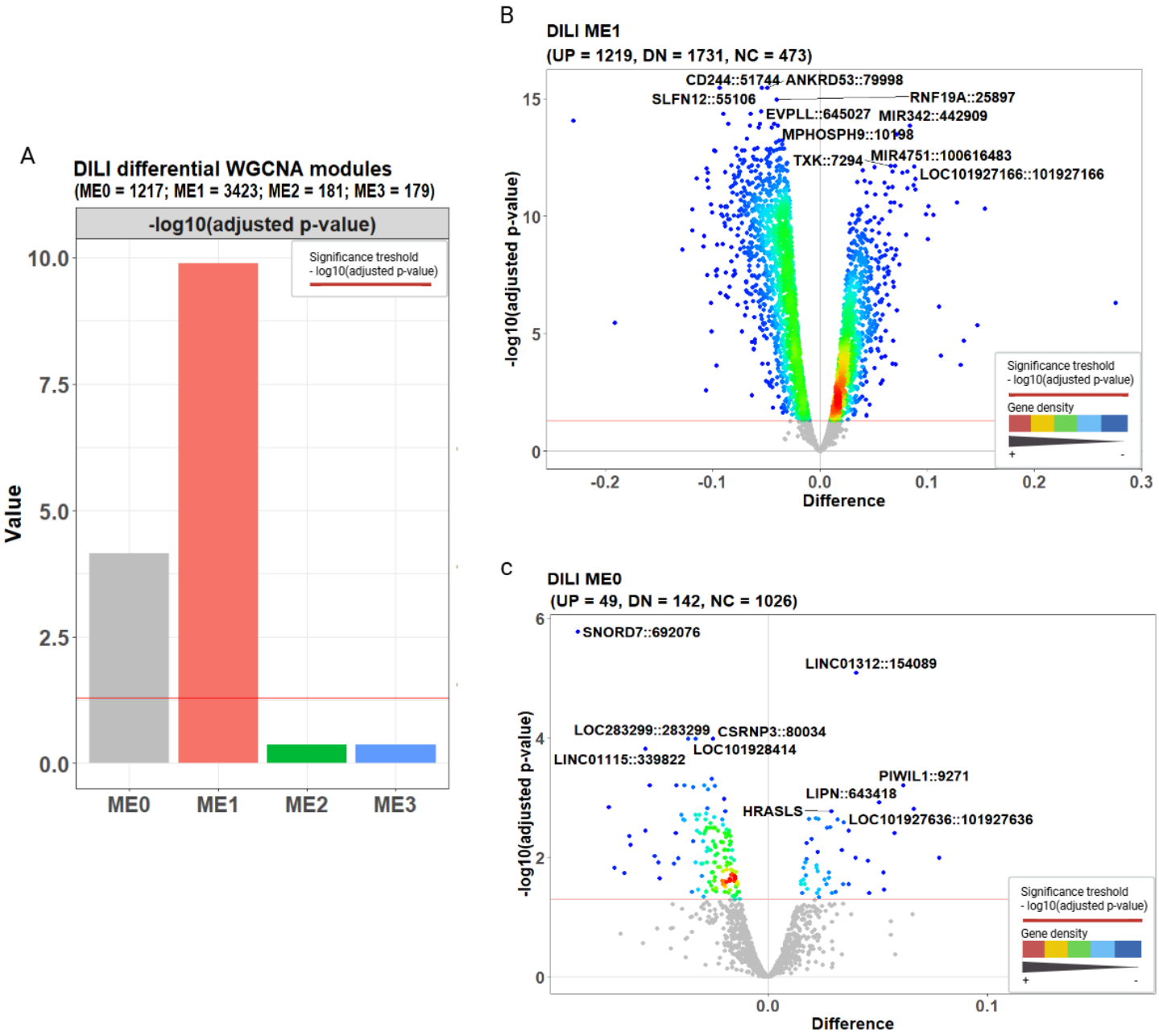


Figure 3

DNA methylation-based WGCNA modules bar plot and differentially methylated genes ME0 and ME1 volcano plots. Methylation-based WGCNA was conducted on gene mean Δβ values of CpG sites located in the TSS1500, TSS200 and the first exon regions as a whole. P-values were FDR adjusted. 3A DILI DNA methylation-based WGCNA gene modules bar plot. 3B ME1 differentially methylated genes volcano plot. 3C ME0 differentially methylated genes volcano plot. In both figures, hypomethylated genes show "difference" or mean Δβ values <0, whereas hypermethylated genes show "difference" or mean Δβ-values >0. Abbreviations: ME0: module 0, ME1: module 1, ME2: module 2, ME3: module 3.

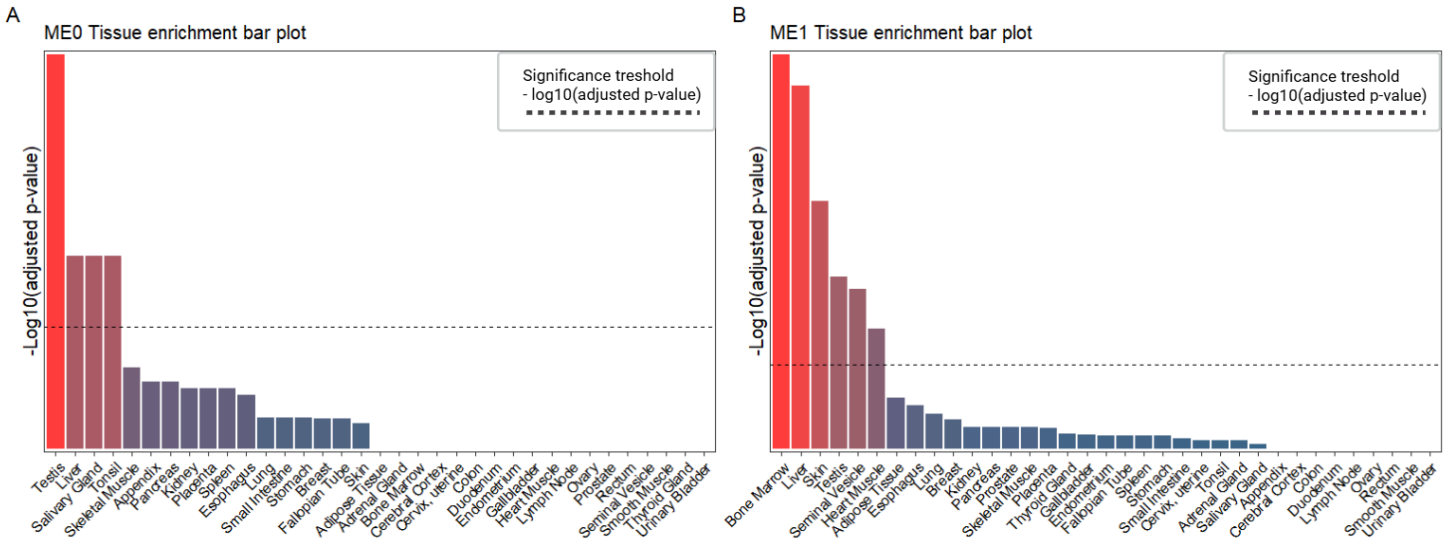


Figure 4

ME0 and ME1 differentially methylated protein-coding genes tissue enrichment bar plot. P-values were FDR adjusted. 4A ME0 differentially methylated protein-coding genes tissue enrichment bar plot. 4B ME1 differentially methylated protein-coding genes tissue enrichment bar plot. Abbreviations: ME0: module 0, ME1: module 1.

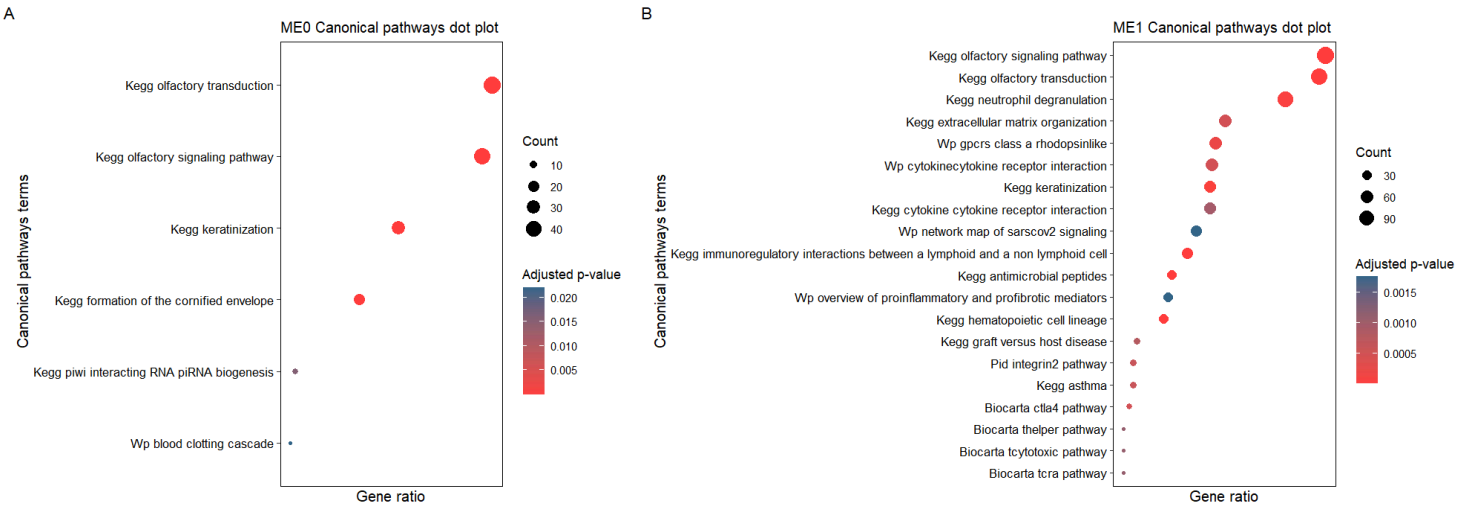


Figure 5

ME0 and ME1 Canonical pathways functional enrichment analysis dot plots. 5A ME0 Canonical pathways functional enrichment analysis dot plot. 5B ME1 top 20 significant Canonical pathways functional enrichment analysis dot plot. Abbreviations: ME0: module 0, ME1: module 1.

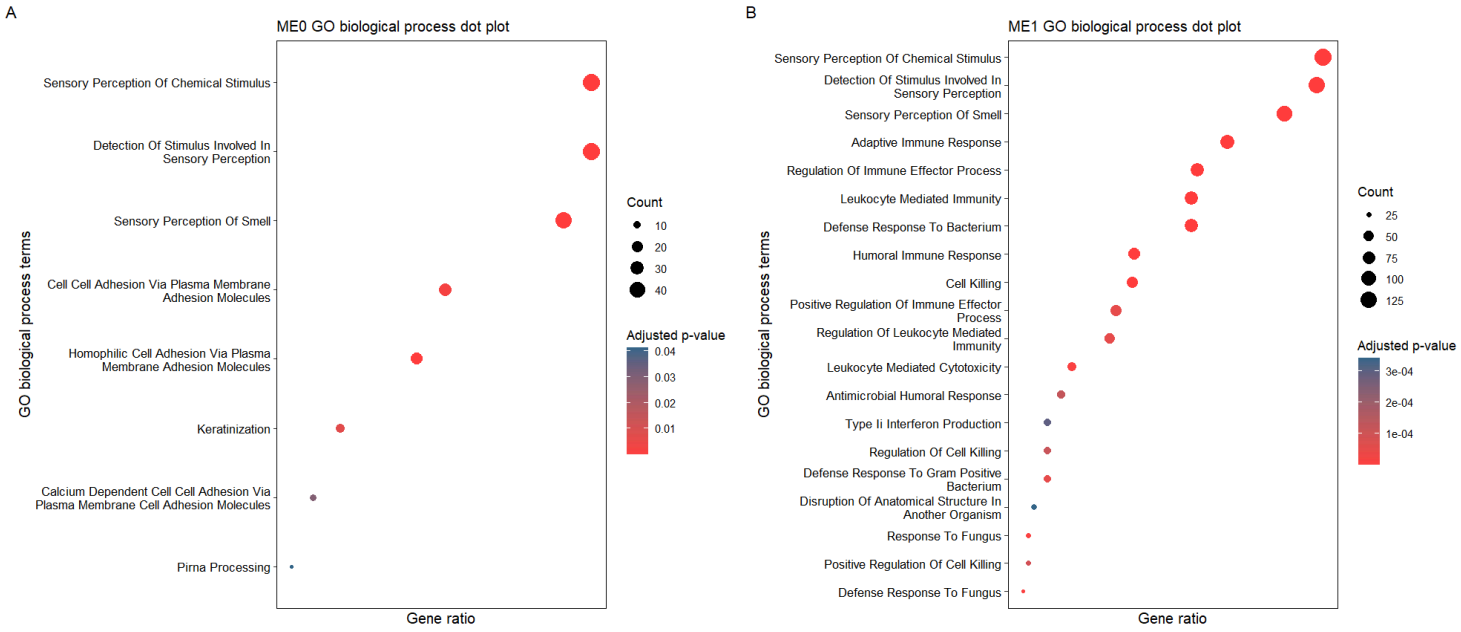


Figure 6

ME0 and ME1 GO biological process functional enrichment analysis dot plots. 6A ME0 GO biological process terms functional enrichment analysis dot plot. 6B ME1 top 20 significant GO biological process terms functional enrichment analysis dot plot. Abbreviations: ME0: module 0, ME1: module 1, GO: Gene Ontology.

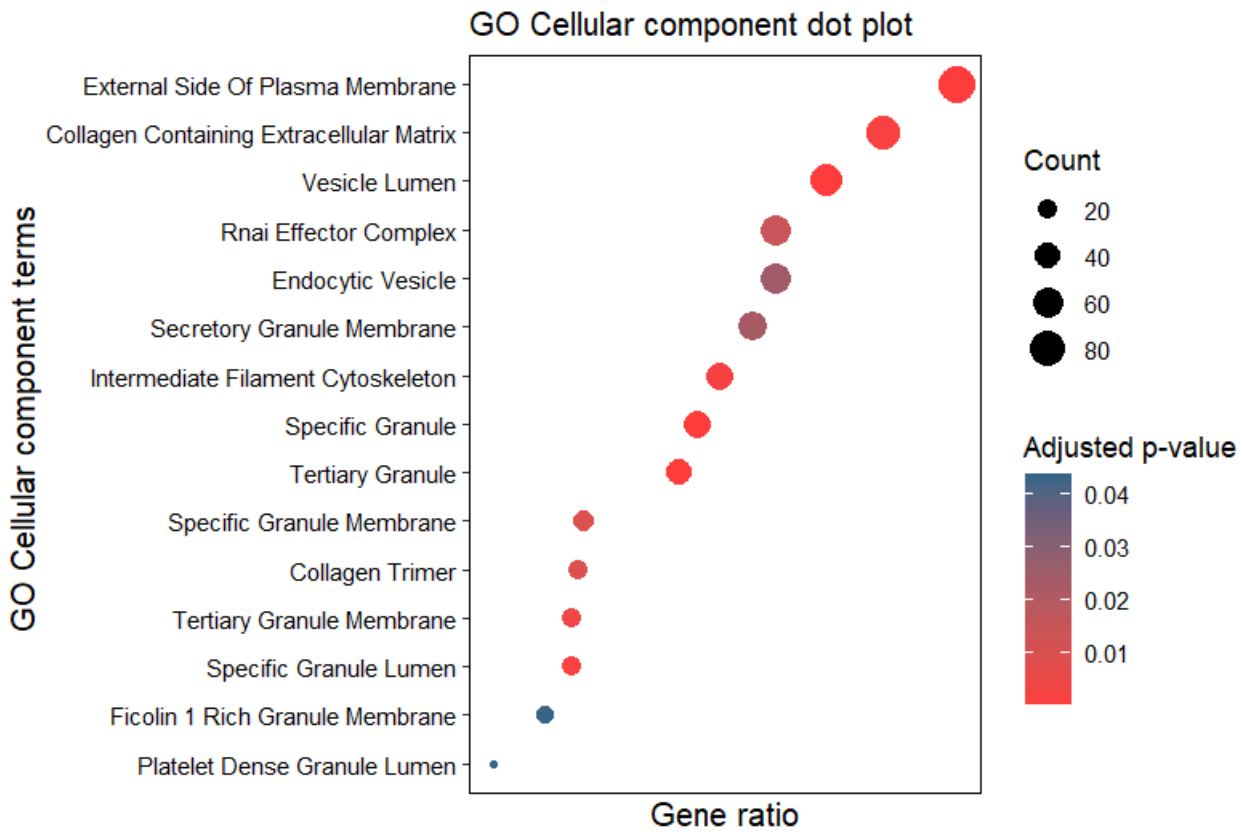


Figure 7

ME1 GO cellular component dot plot. Abbreviations: ME1: module 1, GO: Gene Ontology.

Supplementary Files

This is a list of supplementary files associated with this preprint. Click to download.

- SupplementarymaterialHumanGenomicsDILIMWASWGCNA030326.docx